

Torus Instability in an Extended Medium

Seung Ki BAEK* and Hie-Tae MOON

Department of Physics, Korea Advanced Institute of Science and Technology, Daejeon 305-701

We investigate the dynamics of quasiperiodic solution in a real flow. Here, a two-mode truncation of the Ginzburg-Landau equation is considered entailing a four-dimensional phase space. We analyze, in particular, the evolution and the instability of single-lobed tori observed in the phase space. One-dimensional return maps are used to investigate the basic characteristics of the dynamics.

PACS numbers: 05.45.-a

Keywords: Ginzburg-Landau equation, Torus instability

I. INTRODUCTION

We consider a continuous physical system where a monochromatic wave is modulationally destabilized. The slow temporal and spatial modulation of the envelopes of a destabilized wave train, in a weakly nonlinear medium, is universally described by the Ginzburg-Landau equation (GL):

$$\Psi_t = \epsilon\Psi + (\epsilon + i)\Psi_{xx} - (\epsilon - i)|\Psi|^2\Psi, \quad (1)$$

where the real positive parameter ϵ measures the strength of dissipation of the system. GL first arose in the context of superconductor theory, but now it is known that fluid-dynamics problems such as Rayleigh-Bénard convection and Taylor vortex flow, pattern forming and many reaction-diffusion systems are governed by this equation [1–5]. GL has been extensively studied, due to its pervasiveness in various fields.

Ref. [6] accounts for the numerically observed exponential decay of the Fourier modes. In other words, the distance between the solution of GL and that of its N th order Fourier-mode approximation becomes exponentially small as N increases. This result explains that the GL equation can be approximated by low dimensional Galerkin projections. Three-dimensional truncation, however, fails to mimic many of the details of the full GL equation because the truncation lacks many of the same homoclinic orbits [7,8]. Hence, the dimension of the approximated equation should be at least four.

Following Ref. [8], we analyze bifurcations in the sub-dynamical system obtained by restricting the GL to the space of even functions \mathcal{E} ; solutions for this restricted system can always be expressed as a cosine series under periodic boundary conditions [9]:

$$\Psi(x, t) = a_1(t) + a_2(t) \cos qx + a_3(t) \cos 2qx + \dots, \quad (2)$$

where $a_i(t)$ are complex. Note that Eq. (1) has an odd power nonlinearity which guarantees that an even

(or odd) initial condition should result in an even (or odd) solution. Two complex modes are chosen near the threshold of modulational instability, entailing a four-dimensional phase space [10]:

$$\begin{aligned} a_1 &= \epsilon a_1 + (i - \epsilon) \left\{ |a_1|^2 a_1 + a_1 |a_2|^2 + \frac{1}{2} a_1^* a_2^2 \right\}, \\ a_2 &= \epsilon a_2 - q^2(i + \epsilon) a_2 \\ &\quad + (i - \epsilon) \left\{ a_1^2 a_2^* + 2|a_1|^2 a_2 + \frac{3}{4} |a_2|^2 a_2 \right\}. \end{aligned} \quad (3)$$

Eq. (3) contains two parameters ϵ and q , which measure the strength of dissipation and spatial frequency, respectively. When $\epsilon = 0$, the system becomes conservative, and the $O(2)$ symmetry of Eq. (1) still remains as an inversion symmetry $a_2(t) \rightarrow -a_2(t)$, which plays an active role such as symmetry breaking and restoration in dynamic evolution.

As is well-known, Eq. (3) possesses a limit cycle solution, usually called Stokes mode, with frequency $\omega = 1$:

$$a_1(t) = e^{it}, \quad (4)$$

regardless of ϵ and q . How this mode loses or gains stability is a matter of particular importance. A linear stability analysis shows that it becomes unstable under the following perturbation if ϵ is small:

$$\begin{aligned} a_1(t=0) &= 1, \\ a_2(t=0) &= \delta \ll 1, \end{aligned} \quad (5)$$

if $q \leq q_{th} \approx \sqrt{2}(1 - \epsilon^2)$. Now let us see how Eq. (5) becomes structurally destabilized at various ϵ 's. This system displays plenty of dynamics as we explore the parameter space.

The main purpose of this paper is to present the bifurcation phenomena by using nonlinear dynamical tools and to clarify the relationship with the classical examples, such as the Lorenz system and the logistic map. Then, as those systems serve as touchstones of many theories in lower than four dimensions, Eq. (3) may

*E-mail: garuda@kaist.ac.kr

be another case in four dimensions. The results below show that the dissipation ϵ strongly affects the stability of single-lobed tori, which is critical in the whole bifurcation history [11,12], and that the characteristic behaviors can be simulated by simple and familiar one-dimensional return maps, in spite of the high dimensionality.

II. BEHAVIORS OF A FOUR-DIMENSIONAL SYSTEM

One can write a_1 in polar form:

$$a_1(t) = e^{i\theta(t)}|a_1(t)|, \quad (6)$$

and Eq. (1) has the S^1 phase symmetry:

$$(\alpha \cdot \Psi)(x, t) = \Psi(x, t)e^{i\alpha}, \quad (7)$$

where α is real. This phase symmetry allows a simple choice of coordinates on \mathcal{E} , decoupled from $\theta(t)$. We correlate movement of this system with the solution amplitude because taking amplitude removes phase information. Ref. [13] investigated dynamical features of GL in use of K_i , the i th maximum of $|a_2|$.

Another approach rewrites the trajectory as follows:

$$\begin{aligned} a_1 &= 1 - Z(t) + iW(t), \\ a_2 &= X(t) + iY(t), \end{aligned} \quad (8)$$

to obtain a 4-dimensional phase space spanned by X , Y , Z , and W . Since we cannot visualize trajectories in 4-dimensional space, we study the corresponding discrete trajectories in a 3-dimensional Poincaré space defined properly: whenever a trajectory passes through the plane $W = 0$ with a direction $dW/dt > 0$, we mark the other three coordinates (X, Y, Z) of the piercing point. The n th point (X_n, Y_n, Z_n) is then uniquely mapped into the next point $(X_{n+1}, Y_{n+1}, Z_{n+1})$, which now defines a discrete trajectory in a 3-dimensional space, which we refer to here as the Poincaré space.

1. Large dissipation ($\epsilon = 0.40$)

Figure 1(a) and (b) depict the bifurcation diagram of K_i and the Poincaré sections of Eq. (3), respectively. In this case, the whole bifurcation history appears as a simple continuous line, since the large dissipation suppresses all sudden transitions. The origin, representing the Stokes mode, loses its stability at $q \simeq 1.204$ via supercritical pitchfork bifurcation, and another periodicity (I) becomes a new solution breaking the inversion symmetry. After this periodicity undergoes Hopf bifurcation yielding a single-lobed torus (II), it in turn bifurcates into a double-lobed torus (II') on touching the origin with $q \simeq 0.950$ (Figure 1(b)).

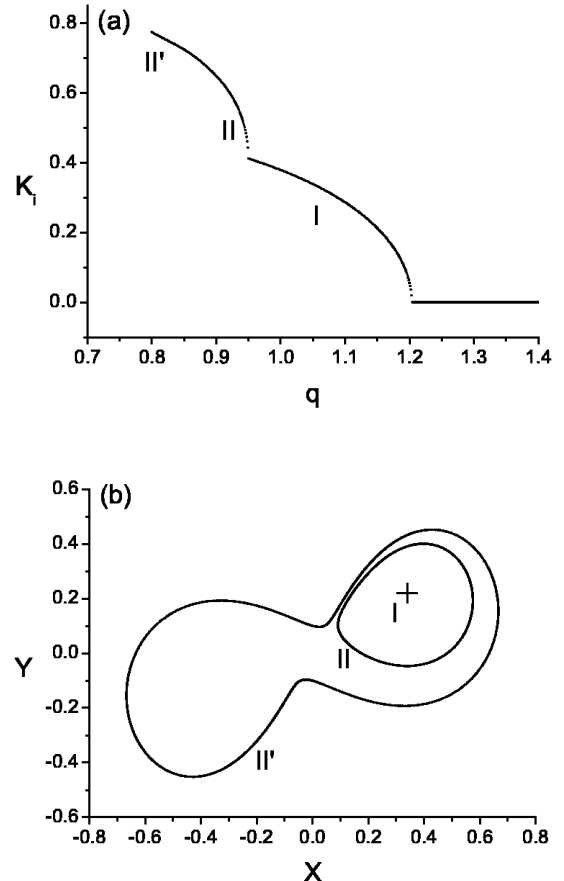


Fig. 1. A large-dissipation case of $\epsilon = 0.40$ with (a) the bifurcation diagram in terms of $|K_i|$, and (b) a Poincaré section. I: an asymmetric periodic orbit marked by a cross; II: a single-lobed torus; III: a double-lobed torus.

One of the authors explained the creation of the torus as being guided by repelling invariant manifolds of three fixed points in the Poincaré space [10]: the origin is a saddle and its unstable manifolds guide the trajectory into a torus. Ref. [14] explains that the symmetry should be restored immediately at the moment when an asymmetric orbit, a single-lobed torus, comes into contact with a symmetric point, the origin.

2. Small dissipation ($\epsilon = 0.06$)

If the dissipation is small, the bifurcation diagram exhibits a discontinuous transition (Figure 2(a)). The asymmetric periodicity (I) jumps up to a double-lobed torus (II) at $q \simeq 1.121$ via subcritical Hopf bifurcation.

If we move the control parameter q in the other direction, the cycle enters the route to chaos via period-doubling cascade (Figure 2(b)). The bifurcation sequence, which is common in many dynamical systems,

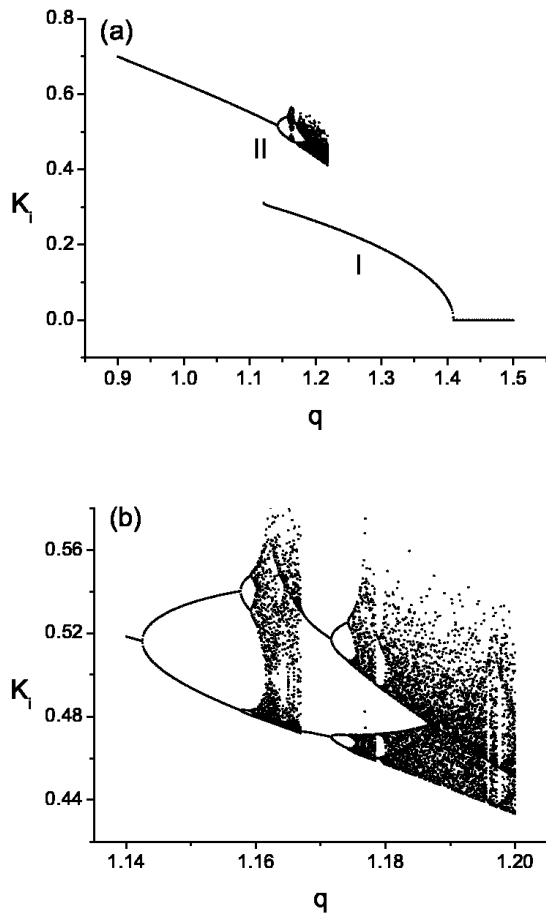


Fig. 2. A small-dissipation case of $\epsilon = 0.06$ with (a) the bifurcation diagram, and (b) the enlarged period-doubling cascade. The single-lobed torus disappears in this figure by losing its stability.

starts with breaking the inversion symmetry, doubles its period, and restores symmetry when it finally becomes chaotic. This pattern repeats itself three times, where the starting periods are 1, 2, and 4, respectively. Plotting (K_i, K_{i+1}) , we observe a noninvertible one-dimensional return map at the chaotic region, similar to that of the Lorenz system. These chaotic behaviors end with $q \simeq 1.218$, and the system returns back to periodicity (I). Since this kind of phenomenon is highly nontrivial, we denote it as *complex hysteresis* [15]. The single-lobed torus is now unstable and thus plays a role of borderline between the basins of attraction for periodicity and chaos.

3. Intermediate dissipation ($\epsilon = 0.21$)

Figure 3 describes an intermediate stage between large and small dissipation. Now we see the emergence of a sta-

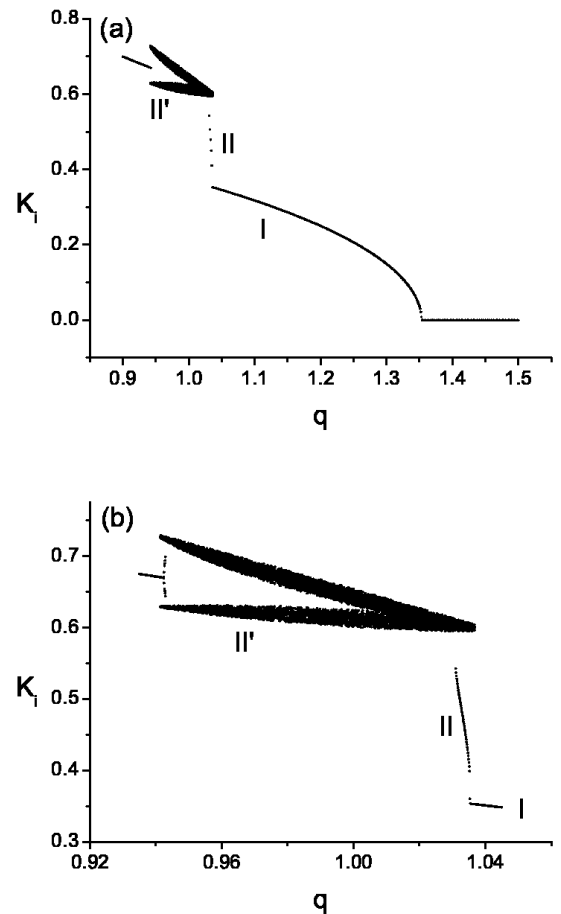


Fig. 3. An intermediate-dissipation case of $\epsilon = 0.21$ with (a) the bifurcation diagram, and (b) the enlarged chaotic region. Note that the Hopf bifurcation becomes supercritical, as the line II indicates.

ble line (II) as in the highly dissipative case. This new connecting branch indicates that the subcritical Hopf bifurcation changes into a supercritical one.

The intermediate value of $\epsilon = 0.21$ pushes the chaotic region (II') to the left and compresses the period-doubling cascade into a single point. Hence if we successively increase q , the torus undergoes period doubling at a single point $q \simeq 0.942$. Such a direct transition from quasiperiodicity to chaos coincides with the result of Ref. [10]. In the other direction with decreasing q , the chaotic orbit persists until $q \simeq 0.940$ and then a torus is suddenly recovered with discontinuity [16].

III. DISCUSSION

Despite its simplified aspects, a one-dimensional map is a useful tool for explaining dynamics of high-dimensional systems, especially when they are highly dis-

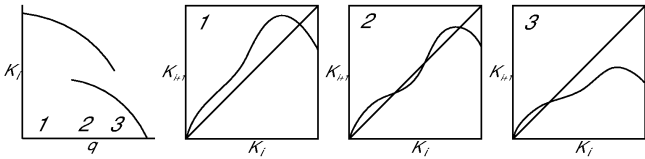


Fig. 4. A simple bistable map. As the control parameter modulates, the map alternates among 1, 2, and 3, exhibiting hysteresis.

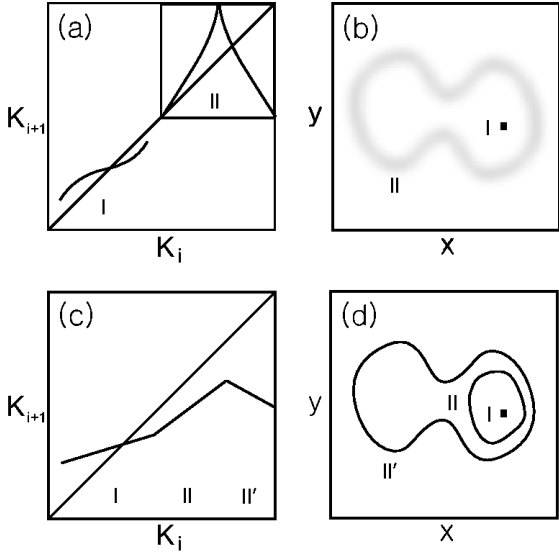


Fig. 5. Schematic diagrams for one-dimensional simplification of Eq. (3). (a) The composite map of a simple intersection and a Lorenz-like cusp for a small-dissipation case, and (b) its corresponding Poincaré section. I: periodicity; II: chaos. (c) A flattened map consisting of three parts, and (d) its corresponding Poincaré section. I: periodicity; II: a single-lobed torus; II': a double-lobed torus.

sipative [17–20].

We first consider a bistable one-dimensional map (Figure 4). As the control parameter changes, it exhibits hysteresis between two stable fixed points. The hysteresis of Eq. (3) is, however, a little different. Let $K_{i+1} = F(K_i)$ denote the one-dimensional return map of this system. On comparing it with the above simple hysteretic map, the main difference is that the upper intersection is replaced by a Lorenz map (Figure 5). Therefore, this system can possess two states, a fixed point and a Lorenz-like chaotic motion. In Ref. [15], we suggested a complex hysteresis map as follows (Figure 6):

$$F(x) = qh(x; \kappa_1, \sigma_1) + (1 - q)h(x; \kappa_2, \sigma_2) \quad (9)$$

with $(\kappa_1, \sigma_1) = (0.4, 0.07)$ and $(\kappa_2, \sigma_2) = (0.6, 0.3)$, where

$$h(x) = \kappa x^{1/3} + 0.67x^2 \exp \left\{ -\left(\frac{x - 0.72}{\sigma} \right)^2 \right\}. \quad (10)$$

According to Ref. [20], each part of the Lorenz map is

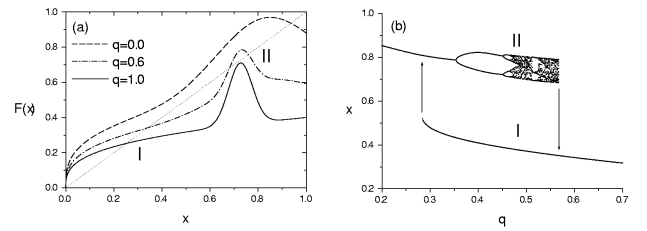


Fig. 6. (a) The map F in Eq. (9), and (b) its bifurcation diagram simulating the result of Figure 2.

interpreted geometrically on the original Lorenz system. That is, the cusp corresponds to a homoclinic trajectory in the real flow which terminates in the origin and the contact point with the 45-degrees line represents Hopf periodic points, where single-lobed tori arise. Similar statements also apply to our system, due to the genericity of the Lorenz model [21,22]. The Hopf bifurcation point is unstable ($|F'| > 1$), and the orbit is immediately thrown into the chaotic Lorenz map as soon as it arrives at the Hopf bifurcation.

The map approach gives another insight on this system. It is well known that a one-dimensional map can be partitioned by choosing critical points. Henceforth, each side of the cusp is given a different symbol. The right partition is orientation-reversing (OR) and an OR branch causes period-doubling [23], since a symbol sequence is transformed as $11 \rightarrow 11 \rightarrow 10$ by applying OR, where the upper bar means conjugation. Therefore, a period doubles in this manner: $(10)^\infty \rightarrow (1010)^\infty \rightarrow (\bar{1}\bar{0}\bar{1}\bar{0})^\infty \rightarrow (1100)^\infty$. On considering that the OR branch lies outside of the cusp (a homoclinic orbit), this mapping viewpoint explains why period doubling occurs only in the double-lobed torus.

As ϵ increases, the return map becomes lower and flatter, which causes the period-doubling cascade to shrink into a point, as observed in Figure 3. This phenomenon is typical of piecewise linear chaotic systems [24,25]. One can deduce that the map looks like a tent map at $\epsilon = 0.26$ and mainly consists of three parts (Figure 5(c)), all of which have a slope of magnitude less than 1. Then, the left part (I) corresponds to periodicity, the middle part (II) means a single-lobed torus after Hopf bifurcation, and the right part (III) is involved in the appearance of a double-lobed torus. As this map intersects the 45-degrees line stably all the time, there are no jumps, nor chaos.

IV. SUMMARY

We observed various behaviors in the approximated GL resulting from two complex modes truncation. When the dissipation is sufficiently small, single-lobed tori lose stability and the whole bifurcation history also changes quantitatively. A distinctive observation is complex hys-

teresis, *i.e.* subcriticality involving many dynamical states as well as chaos. A one-dimensional map is exploited to describe these phenomena, and this provides a consistent understanding of other previous work.

REFERENCES

- [1] A. C. Newell and J. A. Whitehead, *J. Fluid Mech.* **38**, 279 (1969).
- [2] Y. Kuramoto and T. Tsuzuki, *Prog. Theor. Phys.* **54**, 687 (1975).
- [3] E. M. Lifshitz and L. P. Pitaevskii, *Statistical Physics*, (Oxford, Pergamon, 1980), p. 178.
- [4] J. Yeo and M. K. Ko, *J. Korean Phys. Soc.* **42**, 178 (2003).
- [5] I. N. Askerzade, *J. Korean Phys. Soc.* **43**, 111 (2003).
- [6] A. Doelman and E. S. Titi, *Numer. Funct. Anal. and Optimiz.* **14**, 299 (1993).
- [7] A. Doelman, *Nonlinearity* **4**, 231 (1991).
- [8] B. P. Luce, *Physica* **84D**, 553 (1995).
- [9] H-T. Moon, *Phys. Rev. Lett.* **64**, 412 (1990).
- [10] H-T. Moon, *Phys. Rev. Lett.* **79**, 403 (1997).
- [11] W. Lim and S-Y. Kim, *J. Korean Phys. Soc.* **46**, 642 (2005).
- [12] W. Lim and S-Y. Kim, *J. Korean Phys. Soc.* **47**, 414 (2005).
- [13] H-T. Moon, *Phys. Lett.* **325A**, 324 (2004).
- [14] A. Ben-Tal, *Physica* **171D**, 236 (2002).
- [15] S. K. Baek and H-T. Moon, to appear in *Phys. Lett. A*. (DOI): 10.1016/j.physleta.2005.11.053
- [16] To tell a bifurcation delay from hysteresis, we can make use of the fact that the delay is easily broken by a slight perturbation. The observations turn out to be persistent against a dynamical noise.
- [17] J. A. Yorke and E. D. Yorke, *J. Stat. Phys.* **21**, 263 (1979).
- [18] C. Tresser and P. Coullet, *J. Phys. Lettres* **41** L243 (1980).
- [19] S. Fraser and R. Kapral, *Phys. Rev. A* **25** 3223 (1982).
- [20] C. Sparrow, *The Lorenz Equations: Bifurcations, Chaos, and Strange Attractors* (Springer, New York, 1982), p. 234.
- [21] B. A. Malomed and A. Nepomnyashchy, *Phys. Rev. A* **42**, 6238 (1990).
- [22] M. Clerc, P. Coullet and E. Tirapegui, *Phys. Rev. Lett.* **83**, 3820 (1999); *Prog. Theor. Phys. Suppl.* **139**, 337 (2000); *Int. J. Bif. Chaos* **11**, 591 (2001).
- [23] R. Gilmore, *Rev. Mod. Phys.* **70**, 1455 (1998).
- [24] W-M. Zheng and B-L. Hao, *Int. J. Mod. Phys. B* **3**, 1183 (1989).
- [25] P. Cvitanović, G. H. Gunaratne and I. Procaccia, *Phys. Rev. A* **38**, 1503 (1988).